Laboratory #2: HVAC

Logan B. Freeman[1]
MAE 4400 – Thermo-fluids labs, Logan, UT, 84322, USA

Abstract

This experiment evaluates the efficiency of HVAC components using a laboratory air conditioning unit with pre-heater, boiler, and post-heater elements. The study investigates individual component efficiencies and their interactions under five different operational configurations. Measurements of wet and dry bulb temperatures at four system locations enabled psychrometric analysis to determine enthalpy, humidity ratio, and mass flow rates. The experimentally measured efficiencies were 1.75 for the pre-heater, 0.83 for the boiler, and 1.32 for the post-heater, with high measurement uncertainties averaging approximately 0.58 across all components. Results showed that component interactions generally reduced efficiency, with the post-heater's performance dropping from 1.39 when operating alone to 0.59 when all components were active. Overall system efficiency similarly decreased from 1.42 to 1.03 with multiple active elements. Measurement uncertainties, primarily stemming from temperature readings and psychrometric calculations, limited result reliability. Suggested experimental improvements include flow meters for direct mass flow measurement, current meters for power consumption monitoring, and digital thermocouples for more precise temperature readings. Results provide insights into HVAC component interactions while highlighting the challenges of precise efficiency measurement in complex thermal systems.

Nomenclature

d,D = diameter and size of orifice and duct
g = gravitational acceleration
h = specific enthalpy
HR = humidity ratio
H = height
m = mass
m (with over dot) = mass flow rate
p = pressure
P = power
Q = heat
R = resistance
T = temperature
V = voltage
W = work
η = efficiency
ρ = density
σ = uncertainty

Subscripts

0 = denotes quantity associated with atmospheric value

1,2,3,4 = denotes quantity at station within HVAC

preheater, boiler, postheater = denotes quantity associated with specific heating implement

w = denotes quantity associated with water vapor

[1] Senior, Mechanical & Aerospace Engineering, A02302894

I. Introduction

THE importance of heating, ventilation, and air-conditioning (HVAC) systems has grown since the advent of the industrial age. HVAC systems maintain livable conditions inside buildings, automobiles, subway systems, and other edifices of modern cities. HVAC systems monitor and control the temperature and humidity of these environments. As such, they are essential to maintaining comfortable conditions for working and living.

HVAC systems must be robust enough to handle changing environments. For example, people contribute on average 100W of heat to their environment [1]. The HVAC system must be robust enough to add or remove heat, depending on the number of people in the environment. In addition, the HVAC system must maintain correct pressures in the system, so that air flow into or out of the environment is not disrupted.

HVAC systems include, at a minimum, a heating unit, a cooling unit, a ventilation system, and a thermostat. The heating unit can add heat to the air, and it is commonly a furnace, boiler, or heat pump. The cooling unit removes heat and expels it outdoors. The ventilation system includes ducting and fans to circulate air. The thermostat and accompanying sensors provide the correct temperature and humidity air. The heating and cooling processes, as well as any additional thermodynamic processes, have associated efficiencies. In the interest of minimal energy costs, these efficiencies should be high.

This laboratory experiment analyzes the efficiencies of a laboratory HVAC system. The laboratory system serves as a surrogate for a full-sized environmental HVAC system. The laboratory HVAC system features preheaters, post-heaters, a boiler, and a condenser. However, the condenser was out of service when this experiment was performed, and so data on the AC portion of the HVAC system was unavailable.

In this laboratory experiment, the measured change in enthalpy in the HVAC flow is compared to the power input. In this manner, the HVAC efficiency is obtained. Enthalpy is quantified based on wet- and dry-bulb temperature measurements in the flow. The effects of the preheater, post-heater, and boiler on each other are analyzed carefully to determine any impacts to the efficiency.

An uncertainty analysis is performed on the experiment. The uncertainty of the results allows for conclusions to be drawn about the overall efficiency of the HVAC system. The uncertainty contribution from each component of the experimental setup is analyzed to determine possible future improvements on the experimental procedure.

II. Methods

HVAC System Schematic

As described in the Introduction, this experiment will be performed on a laboratory HVAC unit. The model in question is the P. A. Hilton Air Conditioning Laboratory Unit A660. A picture of the A660 unit and schematic are provided below:

Figure 1: Air Conditioning Laboratory Unit A660 as set up in laboratory space [2]

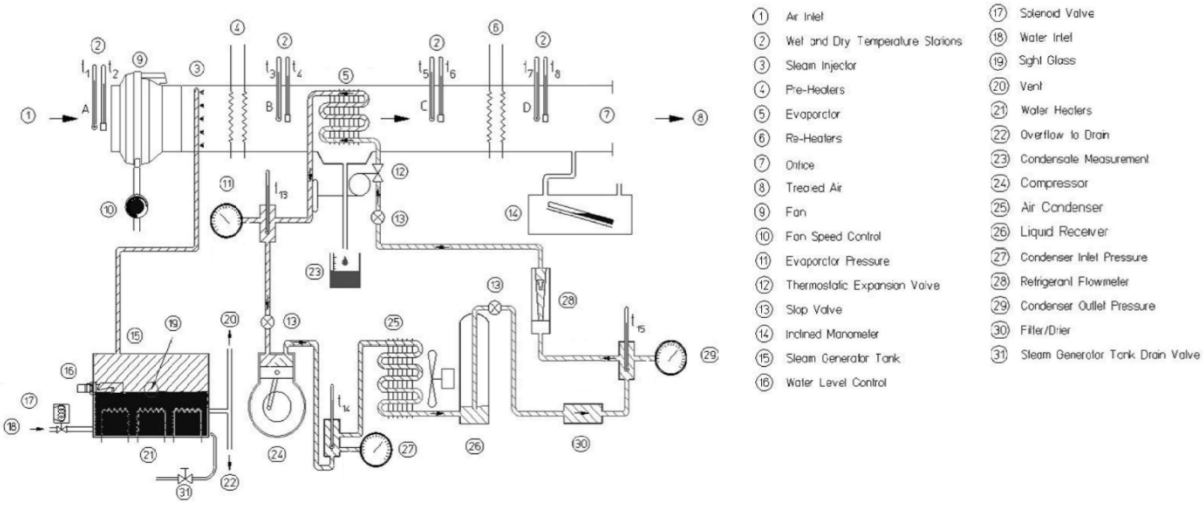

Figure 2: Air Conditioning Laboratory Unit A660 overall system schematic [2]

In this experiment, only the preheater, boiler, and postheater are under investigation. Therefore, the relevant simplified schematic is:

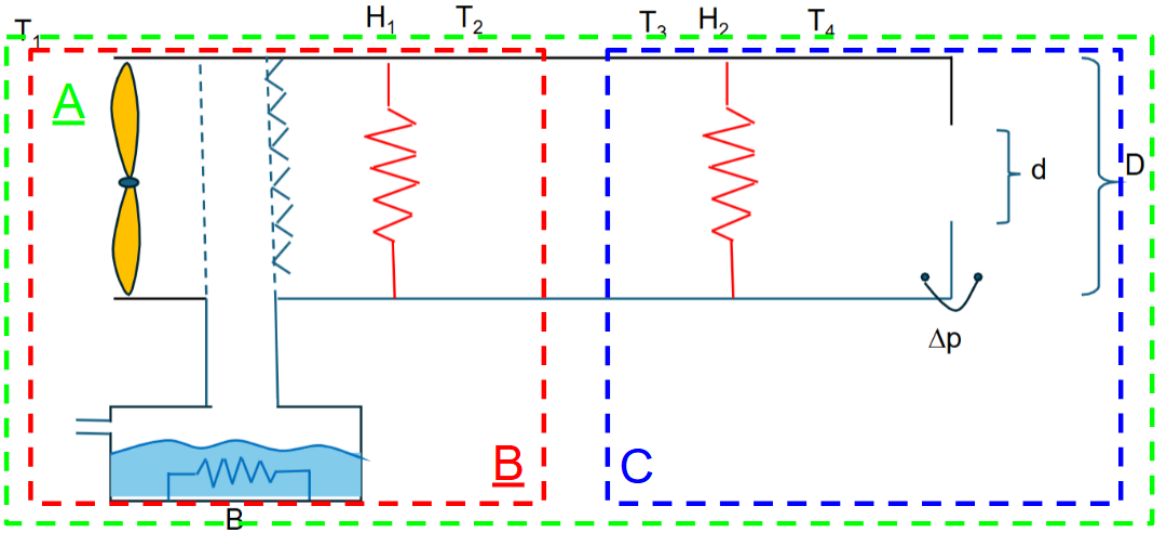

Figure 3: Simplified schematic of laboratory HVAC system. Modified from[2]

In the above figure, three control volumes are outlined with dashed lines. The first is control volume A, outlined in green. It includes the entire HVAC system. The second is control volume B, outlined in red. It includes the boiler and pre-heater. The third is control volume C, outlined in blue. It includes the post-heater.

The fan is always on during the experiment. The fan accelerates the air through the HVAC system, which enables the experiment. Because it performs work on the air stream, the fan contributes to the heating of the air. In particular, the added flow energy dissipates into heat due to viscous effects. However, this effect is negligible.

The HVAC duct is a square channel with side length 0.254m. The duct area is assumed to be constant throughout the duct. The exit orifice is circular with a diameter of 0.1524m. Uniform flow throughout the duct and exit is also assumed.

The duct is instrumented with wet- and dry-bulb thermometers, as well as a manometer. The positions of the thermometer pairs are indicated in Fig. 3. The wet thermometers have a wick cloth wrapped around the bottom to ensure that they stay moist. One end of the wick is suspended in a container of water to ensure the wetness is maintained. The fourth dry thermometer at the exit is replaced with a thermocouple. The thermocouple has a higher maximum temperature. Using a regular dry thermometer at the exit would oversaturate the thermometer. The manometer uses a water column to measure the pressure difference between the flow and the atmosphere.

Psychrometric Calculations

Each wet-dry thermometer pair can be used to quantify the psychrometric conditions in the flow. The psychrometric relations govern humidity, dew point, and enthalpy of air. The conversion from a wet-dry temperature pair to a humidity ratio and enthalpy is performed using a psychrometric chart for an altitude above sea level of 1500m, which is the altitude of Utah State University's campus. An image of a psychrometric chart is included below:

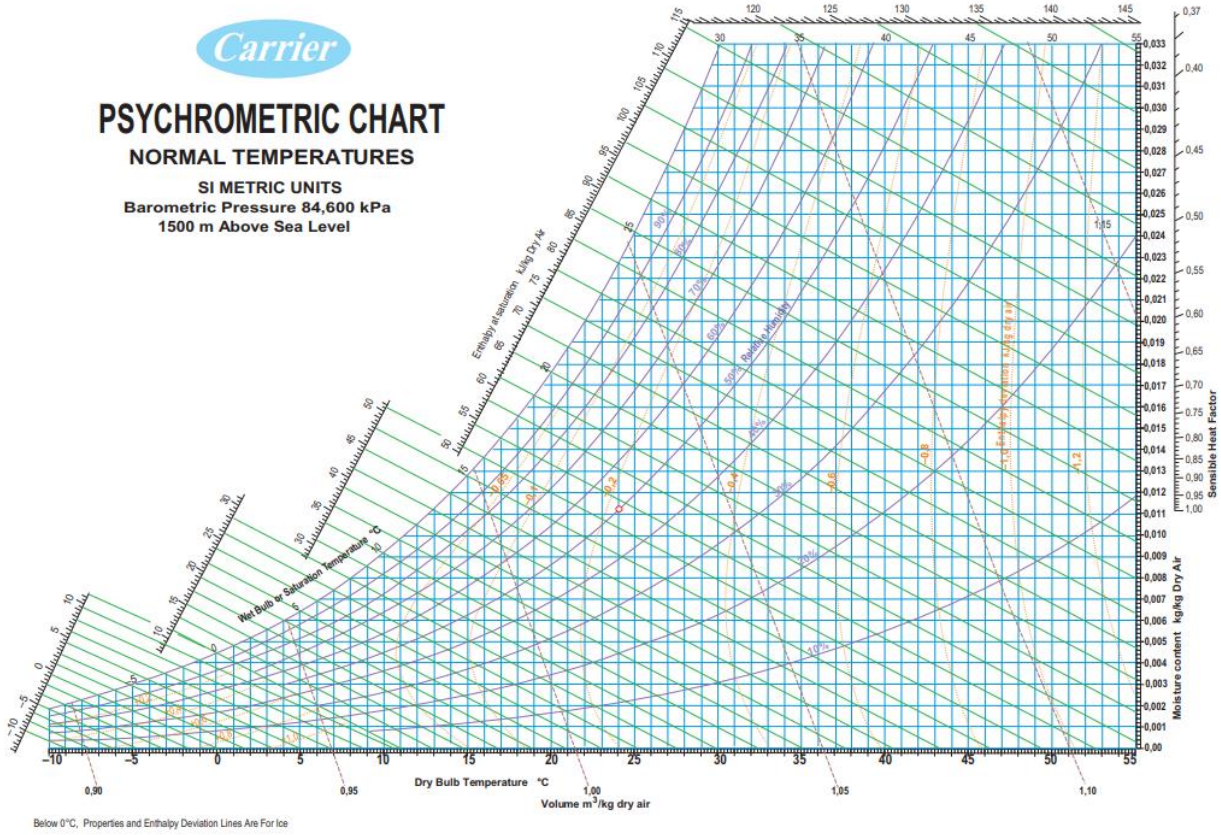

Figure 4: Psychrometric chart for 1500m ASL [2]. The straight diagonal lines correspond with enthalpy and we bulb temperature. The horizontal axis corresponds with dry bulb temperature. The vertical axis corresponds with moisture content.

As will be described below, the dry and wet thermometers can be used to fix the density, enthalpy, and humidity ratio of the flow. The enthalpy in kJ/kg and humidity ratio (HR) in kg/kg can be read straight off the chart. The density is computed with the formula:

$$\rho = \rho_0(1 + HR) \tag{1}$$

The tick marks on the chart are small. As a result, it is sometimes difficult to place the value of a reading exactly. Thus, the uncertainty due to table reading will be considered as one tick mark. Therefore, the uncertainty in enthalpy is 0.5 kJ/kg and the uncertainty in the humidity ratio is 0.0002kg/kg. Assuming the atmospheric density has no uncertainty, the uncertainty in density is calculated as:

$$\sigma_\rho = \rho_0 \, \sigma_{HR} = \rho_0 \tag{2}$$

The atmospheric density is calculated as:

$$\rho_0(T) = 1.00 \frac{kg}{m^3} \frac{293K}{T} \tag{3}$$

These psychrometric values allow for determining the properties of the mixed air-vapor state at each station where there is a wet and dry thermometer. The enthalpy of water vapor is assumed to be constant and is considered to be 2260kJ/kg, with no associated uncertainty.

Experimental Procedure Summarized

A total of five tests are performed, each with a different experimental setup. The tests are described in the table below:

Table 1: Experimental Setup

Test	Boiler Status	Pre-heater Status	Post-heater Status
1	Off	Off	Off
2	Off	Off	On
3	Off	On	On
4	On	On	On
5	On	Off	On

Between each test, sufficient time is allowed for the system to return to equilibrium. Five minutes are allotted after activating or deactivating the pre-heater and post-heater. Ten minutes are allotted after activating the boiler. Each test is described in more detail below.

For all the tests, the fan is run at the lowest possible fan speed that gives a pressure difference of between 6-7 mmH2O. A lower fan speed creates larger changes in temperature from the pre-heater, post-heater, and boiler. The larger changes are easier to observe and quantify. When the pre-heater and post-heater elements are activated, both elements of each are used. When the boiler is used, only the main boiler switch is activated.

Test 1: All off

This test forms a baseline, with all the elements off. The fan is powered on to drive air through the system. The relevant control volume for the first test is control volume A, which includes the entire system. Once the fan has turned on, the system can be considered steady, which means the mass inflow is equal to the mass outflow:

$$\dot{m}_{in} = \dot{m}_{out} \tag{4}$$

Because the boiler is off, the mass inflow is only from the air intake. To calculate the mass flow rate, the change in pressure across the orifice is used. The manometer reading is converted to a pressure difference with:

$$\Delta P = H_{manometer} g \rho \tag{5}$$

which can then be converted into a mass flow rate using:

$$\dot{m}_2 = 0.15\pi \frac{d}{\sqrt{1-\left(\frac{d}{D}\right)^4}} \sqrt{2\rho\Delta P} = \ 0.15\pi \frac{d}{\sqrt{1-\left(\frac{d}{D}\right)^4}} \sqrt{2\rho^2 g} \sqrt{H_{manometer}} \tag{6}$$

In this equation, the only non-constants are the manometer height reading and the density. The density is determined based on the humidity ratio in the psychrometric calculations.

The energy balance is given by:

$$\dot{Q}_{in} - \dot{Q}_{out} + \dot{W}_{in} - \dot{W}_{out} = 0 \tag{7}$$

In the first test, the only engaged appliance is the fan. The fan imparts energy to the flow, and some of the flow energy is converted to heat through viscous dissipation at the wall or in the turbulent structures. However, the heat energy added by the fan is negligible compared to the heaters and boiler and will not be analyzed as contributing to efficiency. Therefore, the first test is only a verification that the thermometers are reading similar conditions. The mass flow can also be computed.

Test 2: Post-heater on

For this test, the post-heater is engaged. The fan remains on. The boiler and pre-heater are off. The system is allowed 5 minutes for the temperature to equilibrate. The control volume for this test is control volume C, between

the second and third thermometers. The fan is running at the same condition throughout the test, so the flow is assumed to be steady. In addition, no mass flow is added, therefore:

$$\dot{m}_{in} = \dot{m}_{out} = \dot{m} \tag{8}$$

The energy balance for the control volume is based on the mass flow rates and the enthalpy difference between the third and fourth thermometers:

$$\dot{m}(h_4 - h_3) = \dot{Q}_{postheater} \tag{9}$$

This equation allows for the calculation of the efficiency with:

$$\eta_{postheater} = \frac{\dot{m}(h_4 - h_3)}{\dot{P}_{postheater}} \tag{10}$$

Test 3: Pre-heater and post-heater on

The third test setup uses both the pre-heater and post-heater. After the pre-heater is turned on, five minutes are allowed for the system to equilibrate. The fan continues running at the same setting. The flow is considered steady once it is at equilibrium. The relevant control volumes are control volume A, B, and C. Control volume A quantifies the overall change, B quantifies the pre-heater, and C relates to the post-heater. No mass is added inside the control volume, so the mass flow is:

$$\dot{m}_{in} = \dot{m}_{out} = \dot{m} \tag{11}$$

The energy balance is expressed in terms of the mass flow rate, enthalpy, and heat added. Energy balances can be expressed for control volumes A, B and C:

$$\dot{m}(h_4 - h_1) = \dot{Q}_{preheater+postheater} \tag{12}$$

$$\dot{m}(h_2 - h_1) = \dot{Q}_{preheater} \tag{13}$$

$$\dot{m}(h_4 - h_3) = \dot{Q}_{postheater} \tag{14}$$

The efficiency can be calculated for the preheater, post-heater, and combination:

$$\eta_{preheater+postheater} = \frac{\dot{m}(h_4 - h_1)}{P_{preheater} + P_{postheater}} \tag{15}$$

$$\eta_{preheater} = \frac{\dot{m}(h_2 - h_1)}{P_{preheater}} \tag{16}$$

$$\eta_{postheater} = \frac{\dot{m}(h_4 - h_3)}{P_{postheater}} \tag{17}$$

The preceding equations refer to control volumes A, B, and C respectively.

Test 4: All on

The fourth test uses the pre-heater, post-heater, and boiler. After the boiler is engaged, ten minutes are allowed for the system to reach equilibrium, since the boiler takes longer to heat up. The fan continues at the same setting. The relevant control volumes are control volumes A, B, and C. Control volume A quantifies the overall change with all three elements. Control volume B quantifies the change of the combined boiler and preheater. Control volume C quantifies the change of the post-heater. Mass is added by the boiler in the form of water vapor. Therefore, the mass balance is:

$$\dot{m}_2 = \dot{m}_3 = \dot{m}_4 = \dot{m}_1 + \dot{m}_w \tag{18}$$

The water mass can be determined with:

$$\dot{m}_w = \dot{m}_2 - \dot{m}_1 = \dot{m}_2 \frac{HR_2 - HR_1}{1 + HR_2} \tag{19}$$

The energy balances in control volumes can be determined by balancing the heat input, which can be determined by measurements and psychrometric calculations:

$$\dot{m}_2 \left(h_2 - \frac{1 + HR_1}{1 + HR_2} h_1 - \frac{HR_2 - HR_1}{1 + HR_2} h_w + h_4 - h_3 \right) = \dot{Q}_{net} \tag{20}$$

$$\dot{m}_2 \left(h_2 - \frac{1 + HR_1}{1 + HR_2} h_1 - \frac{HR_2 - HR_1}{1 + HR_2} h_w \right) = \dot{Q}_{preheater+boiler} \tag{21}$$

$$\dot{m}_2 (h_4 - h_3) = \dot{Q}_{postheater} \tag{22}$$

The above equations are for control volumes A, B, and C respectively. The efficiencies are then calculated with:

$$\eta_{net} = \frac{\dot{Q}_{net}}{P_{boiler} + P_{preheater} + P_{postheater}} \tag{23}$$

$$\eta_{preheater+boiler} = \frac{\dot{Q}_{preheater+boiler}}{P_{boiler} + P_{preheater}} \tag{24}$$

$$\eta_{postheater} = \frac{\dot{Q}_{postheater}}{P_{postheater}} \tag{25}$$

These are for A, B, and C respectively.

Test 5: Boiler and post-heater on

The fifth test turns off the pre-heater and only uses the boiler and post-heater. Five minutes are allowed for the system to return to equilibrium after disengaging the pre-heater. The fan is maintained at the same setting. The relevant control volumes are A, B, and C. Control volume A quantifies the overall change with the boiler and post-heater elements. Control volume B quantifies the change of the boiler. Control volume C quantifies the change of the post-heater. Mass is added by the boiler in the form of water vapor. The mass balance is the same as in the fourth test, and the energy balances for control volumes B, C, and A are reproduced below:

$$\dot{m}_2 \left(h_2 - \frac{1 + HR_1}{1 + HR_2} h_1 - \frac{HR_2 - HR_1}{1 + HR_2} h_w + h_4 - h_3 \right) = \dot{Q}_{net} \tag{26}$$

$$\dot{m}_2 \left(h_2 - \frac{1 + HR_1}{1 + HR_2} h_1 - \frac{HR_2 - HR_1}{1 + HR_2} h_w \right) = \dot{Q}_{boiler} \tag{27}$$

$$\dot{m}_2 (h_4 - h_3) = \dot{Q}_{postheater} \tag{28}$$

The above equations are for control volumes A, B, and C respectively. The efficiencies are then calculated with:

$$\eta_{net} = \frac{\dot{Q}_{net}}{P_{boiler} + P_{postheater}} \tag{29}$$

$$\eta_{boiler} = \frac{\dot{Q}_{preheater+boiler}}{P_{boiler}} \tag{30}$$

$$\eta_{postheater} = \frac{\dot{Q}_{postheater}}{P_{postheater}} \tag{31}$$

Test 5 then allows the direct calculation of the boiler efficiency.

Measurement uncertainties

Each measurement tool has an associated uncertainty. The measurement uncertainty of the thermometers is $\epsilon_T = 0.25C$ for all the thermometers, and the measurement uncertainty for the manometer is $\epsilon_{h,mano} = 0.1mm$. The dimensional measurements of the HVAC duct diameter and orifice diameter are assumed to have zero uncertainty. Therefore, the mass flow rate uncertainty only depends on the experimental measurement uncertainties.

The power is given by:

$$P = \frac{V^2}{R} \tag{32}$$

Therefore, the uncertainty in power depends on the uncertainty of voltage and the uncertainty of resistance. The uncertainty of the provided resistances is assumed to be 0.1 Ohm. The uncertainty of the voltage, which is nominally 220V, is considered as 5V [3].

The conversion of these measurement uncertainties into result uncertainties is described in detail in section IV.

Assumptions and limitations

This HVAC lab makes several key assumptions that affect the results. The control-volume analysis assumes steady conditions during measurements, which is why time is allowed for temperatures to stabilize. The real system still has small fluctuations, especially with the slow-responding boiler. Turbulence and power fluctuations also limit the accuracy of the steady-state assumption. A more accurate manner would be looking at time-averaged flow quantities. The analysis also assumes minimal heat loss to the surroundings between measuring points, which isn't true when temperature differences are large.

The lab assumes manometer readings have a direct connection to airflow rates, but this is an idealized assumption. This limits the usable range of the experiment. The suggested measurement sequence tries to isolate how components affect each other, but thermal inertia means earlier states still impact later measurements. The lab also assumes wet-bulb thermometers stay properly wet throughout testing, so they perfectly measure the wet-bub temperature. In addition, the assumption that effects only propagate downstream is inaccurate, especially at lower fan speeds where thermal and mass diffusion upstream are significant. In the limit as fan speed goes to zero, the effects of diffusion vastly outweigh the effects of diffusion.

III. Results

The experimental setup described in the Methods section provides a framework for analyzing the efficiency of different HVAC system components. A total of five tests were conducted, each with different combinations of activated components as outlined in Table 1. For all tests, the fan was operated at the minimum speed that maintained a pressure difference between 6-7 mmH2O across the system, as measured by the water manometer.

For each test, measurements were taken at four key locations throughout the HVAC system, corresponding to the thermometer pair positions indicated in Figure 3. At each location, both wet-bulb and dry-bulb temperatures were recorded, with the exception of position 4 where a thermocouple replaced the standard dry thermometer due to higher operating temperatures. These temperature pairs allowed for the determination of psychrometric properties using the 1500m ASL psychrometric chart appropriate for Utah State University's altitude.

The data collected from the thermometer pairs was processed using psychrometric calculations to determine the enthalpy, humidity ratio, and density at each measurement point. Uncertainty in chart readings was accounted for as ±0.5 kJ/kg for enthalpy and ±0.0002 kg/kg for humidity ratio. These values, along with pressure measurements from the manometer, enabled the calculation of mass flow rates through the system using the orifice equation.

Between each test, sufficient equilibration time was allowed (5 minutes for pre-heater and post-heater changes, 10 minutes for boiler activation) to ensure steady-state conditions before taking measurements. This approach minimized transitional effects and allowed for the application of steady-state control volume analysis. Mass and energy balances were then calculated for the relevant control volumes (A, B, and C) as defined in the Methods section to determine component efficiencies.

Measurement uncertainties were propagated through all calculations, including ±0.25°C for temperature readings, ±0.1mm for manometer readings, and power uncertainties derived from voltage (±5V) and resistance (±0.1Ω) variations. These uncertainty propagations are detailed in the analysis below.

The following data presents the compiled measurements and derived values for all five test configurations. Each test represents different operating conditions of the HVAC system, allowing for comparative analysis of component efficiencies under various scenarios. Table 2 presents the raw temperature and manometer measurements at each station for each of the five tests. The test configurations were previously described in Table 1.

Table 2 Raw data from five tests

Test	T1 Dry (C)	T1 Wet (C)	T2 Dry (C)	T2 Wet (C)	T3 Dry (C)	T3 Wet (C)	T4 Dry (C)	T4 Wet (C)	Manometer (mmH2O)
1	22.25	11.75	22	12	22	11.5	22.5	11	6.9
2	22.25	11.75	22.5	12	24	12	40.5	15.5	7
3	22.25	11.75	38	17.75	37	17	53.5	19	7.1
4	23	12.5	41.25	27	40	26.5	56.2	27.5	6.9
5	23	12.5	26	23	27.25	23	44.2	25	6.8

The wet and dry temperatures at each station are converted into humidity ratios and enthalpies. In addition, densities are calculated based on the temperatures and humidity ratios. These data are included in the Appendix. From the pressure differential and psychrometric values, a mass flow rate and heating rates inside control volumes A, B, and C can be calculated. These are displayed alongside the uncertainties in Table 3.

Table 3 Processed mass flow rate and heat rates from five tests

Test	Exit mass flow rate (kg/s)	Uncertainty of exit mass flow rate (kg/s)	Heat added in CV B (kW)	Uncertainty of heat added in B (kW)	Heat added in CV C (kW)	Uncertainty of heat added in C (kW)	Heat added in CV A (kW)	Uncertainty of heat added in A (kW)
1	0.0280	0.00044	N/A	N/A	N/A	N/A	N/A	N/A
2	0.0268	0.00041	0.0552	1.184	2.70	1.137	2.762	2.322
3	0.0258	0.00039	3.395	1.142	1.710	1.096	5.106	2.238
4	0.0252	0.00039	4.938	1.104	1.153	1.068	6.092	2.173
5	0.0258	0.00041	1.680	1.134	2.233	1.096	3.914	2.231

The first test does not include calculated values for heat added and uncertainty for the first test, because the only implement which is active is the fan, and the heat added by the fan is negligible and not able to be measured with laboratory equipment. The uncertainty in added heat is driven by the propagation of measurement uncertainties through the enthalpy differential calculations, which rely on psychrometric chart readings and temperature measurements at each station. Mass flow rate uncertainties further compound this effect, because they depend on manometer readings and density values derived from potentially imprecise humidity ratio determinations.

The power and uncertainty in power of the implements is derived from the measured resistances, uncertainty of the resistances, and uncertainty of the voltages. The values for each power are included in the appendix. The values of the total power added to each control volume for each test is displayed below, in Table 4.

Table 4: Power and uncertainty of power

Test	Power B (W)	Uncertainty of Power B (W)	Power C (W)	Uncertainty of Power C (W)	Power A (W)	Uncertainty of Power A (W)
1	0	0	0	0	0	0
2	0		1945.7	88.5	1945.7	88.5
3	1941.8	88.3	1945.7	88.5	3887.6	176.8
4	3975.4	181.1	1945.7	88.5	5921.2	269.7
5	2033.6	92.8	1945.7	88.5	3979.4	181.3

Based on the already displayed values for power and heat added, the efficiency of each control volume can be calculated. The uncertainty of the control volumes is also calculated.

Table 5: Efficiencies of control volumes

Test	Efficiency of B	Uncertainty of B	Efficiency of C	Uncertainty of C	Efficiency of A	Uncertainty of A
2	N/A	N/A	1.391	0.587	1.419	1.195
3	1.748	0.593	0.879	0.564	1.313	0.57
4	1.242	0.283	0.593	0.550	1.028	0.370
5	0.826	0.559	1.148	0.566	0.983	0.562

The overall system efficiency (control volume A) remains relatively consistent across Tests 3-5, hovering near the 1.0 mark, which suggests reasonable energy conversion. However, the unusually high efficiency in Test 2 (1.42) again points to potential measurement issues or unaccounted energy inputs. The uncertainty will be discussed in more depth later. The uncertainties are all high, which is primarily driven by uncertainty in the added heat. Based on the assumption that disturbances do not propagate downstream, the uncertainty of each of the elements can be obtained. These are displayed in Table 6.

Table 6: Efficiency of pre-heater, boiler, and post-heater

	Efficiency	Uncertainty of efficiency
Pre-heater	1.748	0.593
Boiler	0.826	0.559
Post-heater	1.313	0.578

The efficiency analysis of the HVAC components reveals distinct performance characteristics for each element. The pre-heater demonstrates the highest efficiency at 1.75, which exceeds theoretical perfect efficiency and suggests measurement errors or unaccounted heat transfer mechanisms. The boiler shows a more reasonable efficiency of 0.83, indicating some heat loss but generally acceptable performance for this type of system. The heat loss is to the external surroundings, or to the water reservoir. The post-heater's efficiency of 1.31 also exceeds unity, which is physically impossible and points to experimental limitations.

The pre-heater's uncertainty of 0.59, the boiler's uncertainty of 0.56, and the post-heater's uncertainty of 0.58 all represent significant fractions of their respective efficiency measurements. These high uncertainties come from the measurement errors in temperatures, pressure readings, and psychrometric calculations. These propagate through the calculation. Notably, all the efficiencies are within range of 1.0, when considering the uncertainty.

Looking at Table 5, the efficiency values show several notable patterns across the different test configurations. The pre-heater (control volume B) demonstrates particularly high efficiency in Test 3, exceeding 1.7, which suggests it's operating above theoretical perfect efficiency. This counterintuitive result likely indicates measurement errors within the system. The post-heater (control volume C) shows considerable variation, achieving its highest efficiency in Test 2 at approximately 1.39, while dropping significantly to 0.59 in Test 4 when all components are operating.

The overall system efficiency (control volume A) remains relatively consistent across Tests 3-5, hovering near the 1.0 mark, which suggests reasonable energy conversion. However, the unusually high efficiency in Test 2 (1.42) again points to potential measurement issues or unaccounted energy inputs.

The uncertainty values are remarkably high across all tests, often approaching or exceeding the magnitude of the efficiency values themselves. This high uncertainty is primarily driven by the propagation of errors through multiple calculation steps, where each measured parameter (temperatures, pressure differences, humidity ratios) contributes its own uncertainty. The enthalpy calculations from psychrometric charts introduce significant uncertainty, which is then magnified when calculating mass flow rates. Since efficiency calculations involve dividing heat transfer rates (themselves products of mass flow and enthalpy differences) by electrical power inputs, the uncertainties compound substantially. The most extreme case appears in Test 2 for control volume A, where the uncertainty exceeds the measured value, making any conclusions about that particular efficiency highly questionable.

Analyzing component interactions reveals notable efficiency patterns across the test configurations. The post-heater achieves its peak efficiency of 1.39 when operating alone, but drops to 0.88 when the pre-heater is activated, suggesting the pre-heated air reduces its effectiveness. When the boiler is introduced in Test 4, both the pre-heater and post-heater efficiencies decline further to 1.24 and 0.59 respectively. However, turning off the pre-heater while keeping the boiler active (Test 5) allows the post-heater's efficiency to recover to 1.15. The overall system efficiency follows this trend, dropping from 1.41 to 1.03 when all components are operating, indicating that simultaneous operation of multiple heating elements generally leads to reduced system-wide performance. Generally, it is expected that the most efficient operation will be obtained when a component is operating alone.

IV. Uncertainty Calculations

Given an arbitrary function of many variables, the overall uncertainty of the function is given by:

$$\sigma_f = \sqrt{\sum_{i=1}^{n} \left(\frac{\partial f}{\partial x_i} \sigma_{x_i} \right)^2} \tag{33}$$

To obtain the overall uncertainty of the efficiency, multiple intermediate uncertainties will be determined. The uncertainty of the density is based on the uncertainty of the temperature. The uncertainty of the density is then:

$$\sigma_{\rho_0} = \frac{1kg}{m^3} \frac{\sigma_T 293K}{T^2} \tag{34}$$

The uncertainty of the psychrometric quantities h and HR are fixed. The uncertainty of the flow density is then:

$$\sigma_\rho = \sqrt{(1 + HR)^2 \sigma_{\rho_0}^2 + \rho_0^2 \sigma_{HR}^2} \tag{35}$$

The uncertainty in the pressure differential across the manometer is:

$$\sigma_{\Delta P} = \sqrt{\left(g \rho \sigma_{H_{\text{manometer}}} \right)^2 + \left(H_{\text{manometer}} g \sigma_\rho \right)^2} \tag{36}$$

Therefore, the uncertainty of the mass flow exit rate is:

$$\sigma_{\dot{m}_2} = \sqrt{\left(\sqrt{2gH_{\text{manometer}}} \frac{d}{\sqrt{1 - \left(\frac{d}{D}\right)^4}} \rho \sigma_\rho \right)^2 + \left(\frac{\sqrt{2\rho^2 g}}{2\sqrt{H_{\text{manometer}}}} \frac{d}{\sqrt{1 - \left(\frac{d}{D}\right)^4}} \sigma_{H_{\text{manometer}}} \right)^2} \tag{37}$$

The uncertainty in the heat added for control volume B is computed as:

$$\sigma_{Q_B} = \sqrt{\left(\left(h_2 - \frac{1+HR_1}{1+HR_2}h_1 - \frac{HR_2 - HR_1}{1+HR_2}h_w\right)\sigma_{\dot{m}_2}\right)^2 + \left(\dot{m}_2\left(\frac{h_1}{(1+HR_2)^2} - \frac{h_w}{(1+HR_2)}\right)\sigma_{HR_1}\right)^2 + \left(\dot{m}_2\left(-\frac{(1+HR_1)h_1}{(1+HR_2)^2} + \frac{h_w}{(1+HR_2)^2}\right)\sigma_{HR_2}\right)^2 + \left(\dot{m}_2\left(-\frac{1+HR_1}{1+HR_2}\right)\sigma_{h_1}\right)^2 + \left(\dot{m}_2\sigma_{h_2}\right)^2} \quad (38)$$

The uncertainty in the heat added for control volume C is computed as:

$$\sigma_{Q_C} = \sqrt{\left((h_4 - h_3)\sigma_{\dot{m}_2}\right)^2 + \left(\dot{m}_2\sigma_{h_4}\right)^2 + \left(\dot{m}_2\sigma_{h_3}\right)^2} \quad (39)$$

Control volume A includes both control volume B and C. The uncertainty is then calculated in a straightforward manner as:

$$\sigma_{Q_A} = \sqrt{\sigma_{Q_B}^2 + \sigma_{Q_C}^2} \quad (40)$$

The uncertainty of an arbitrary generalized efficiency is calculated as:

$$\sigma_\eta = \eta\sqrt{\left(\frac{\sigma_Q}{Q}\right)^2 + \left(\frac{\sigma_P}{P}\right)^2} \quad (41)$$

For an efficiency which includes multiple devices, for example the pre-heater and boiler, the uncertainty of the power is calculated as the sum of the uncertainties of the powers for the devices:

$$\sigma_P = \sum_i \sigma_{P_i} \quad (42)$$

The uncertainty of power for an element is:

$$\sigma_{P,i} = \sqrt{\left(\frac{2V}{R}\sigma_V\right)^2 + \left(-\frac{V^2}{R^2}\sigma_R\right)^2} \quad (43)$$

In the results section, the relative uncertainty is expressed as a percentage. This percentage is obtained as:

$$\sigma_{\eta,re} = \frac{\sigma_\eta}{\eta} \cdot 100 \quad (44)$$

V. Conclusion

In conclusion, this experiment successfully evaluated the efficiency of three key HVAC components—pre-heater, boiler, and post-heater—under various operational configurations. The pre-heater demonstrated the highest efficiency at 1.75, followed by the post-heater at 1.32, while the boiler showed a more modest efficiency of 0.83. These values indicate that the electric heating elements outperform the water vapor-based boiler system in energy conversion efficiency. However, the high uncertainties associated with these measurements (0.59, 0.58, and 0.56 respectively) highlight significant limitations in the experimental methodology and raise questions about the reliability of the efficiency values.

The experiment revealed important interactions between HVAC components that affect overall system performance. When operating in isolation, the post-heater achieved its peak efficiency of 1.39, but this value decreased to 0.88 when the pre-heater was activated, and further declined to 0.59 when all three components operated simultaneously. This suggests that component interactions generally reduce individual element performance, likely due to changes in temperature differentials and flow conditions. The overall system efficiency showed similar behavior, reaching 1.42 with only the post-heater active but decreasing to 1.03 with all components operating, demonstrating that simpler configurations often yield higher efficiency in this HVAC system.

The high uncertainties observed across all measurements represent a significant limitation of this experiment. With uncertainty values frequently approaching or exceeding 50% of the measured efficiency values, the quantitative results must be interpreted with caution. These high uncertainties stem primarily from the propagation of measurement errors through multiple calculation steps, including temperature readings, psychrometric property determinations, and mass

flow calculations. For more reliable efficiency assessments, future experiments should employ more precise measurement techniques, particularly for temperature and humidity readings, which drive much of the uncertainty in the enthalpy calculations.

A significant improvement to the experimental setup would be the integration of a calibrated flow meter to directly measure mass flow rates, eliminating the need for indirect calculations using manometer readings and psychrometric properties. Current meters installed on the power lines would provide real-time, accurate measurements of electrical power consumption for each heating element, replacing the simplified resistance-based calculations that introduce substantial uncertainty. Digital thermocouples for both dry and wet bulb temperature measurements would dramatically increase precision compared to the manual thermometers used in this experiment.

In relation to the original experimental objectives outlined in the introduction, this study successfully quantified the efficiency of individual HVAC components and their interactions within a laboratory setting. The results provide valuable insights into how component configurations affect overall system performance, though the high measurement uncertainties limit the precision of these findings. Future work should focus on reducing measurement uncertainties and exploring additional component configurations to develop more robust efficiency guidelines for HVAC system design and operation.

Appendix - Full Presentation of Raw Data

Test	T1_wet	T1_dry	T2_dry	T2_wet	T3_dry	T3_wet	T4_dry	T4_wet
1	11.75	22.25	22	12	22	11.5	22.5	11
2	11.75	22.25	22.5	12	24	12	40.5	15.5
3	11.75	22.25	38	17.75	37	17	53.5	19
4	12.5	23	41.25	27	40	26.5	56.2	27.5
5	12.5	23	26	23	27.25	23	44.2	25

Test	h1	uncertainty of h1	h2	uncertainty of h2	h3	uncertainty of h3	h4	uncertainty of h4
1	37.63159	0.5	38.34	0.5	36.95	0.5	35.58	0.5
2	37.63159	0.5	38.33	0.5	38.3	0.5	48.4	0.5
3	37.63159	0.5	56.04	0.5	53.46	0.5	60.08	0.5
4	39.72609	0.5	96.36	0.5	93.77	0.5	98.35	0.5
5	39.72609	0.5	77.41	0.5	77.36	0.5	86	0.5

Test	HR1		HR2		HR3		HR4	
1	0.006	0.0002	0.0064	0.0002	0.0058	0.0002	0.0051	0.0002
2	0.006	0.0002	0.0062	0.0002	0.0056	0.0002	0.003	0.0002
3	0.006	0.0002	0.0069	0.0002	0.0063	0.0002	0.0024	0.0002
4	0.0065	0.0002	0.0213	0.0002	0.0208	0.0002	0.016	0.0002
5	0.0065	0.0002	0.0201	0.0002	0.0196	0.0002	0.0161	0.0002

Test	density 1	uncertainty	rho 2		rho 3		rho 4	
1	0.988142	0.001581	0.99	0.001584	0.99	0.001584	0.99	0.001584
2	0.988142	0.001581	0.99	0.001584	0.99	0.001584	0.94	0.001504
3	0.988142	0.001581	0.94	0.001504	0.95	0.00152	0.9	0.00144
4	0.985443	0.001577	0.93	0.001488	0.93	0.001488	0.89	0.001424
5	0.985443	0.001577	0.97	0.001552	0.97	0.001552	0.92	0.001472

Test	m2	uncertainty	QA	QB	QC	Uncertainty of Qb	Uncertainty of Qc
1	0.028026	0.000441					
2	0.026802	0.000415	2.776	0.069	2.707	1.1849	1.1371
3	0.025844	0.000394	5.9557	4.2448	1.7109	1.1421	1.0965
4	0.025195	0.000395	7.3274	6.1734	1.1539	1.1046	1.0689
5	0.025855	0.000411	4.3341	2.1002	2.2339	1.1342	1.0969

Power & Uncertainty

Test	Power B	Uncertainty	Power C	Uncertainty	Power A	Uncertainty
1	0	0	0	0	0	0
2	0		1945.746	88.52945	1945.746	88.52945218
3	1941.874	88.35294	1945.746	88.52945	3887.621	176.882393
4	3975.488	181.184	1945.746	88.52945	5921.234	269.713446
5	2033.613	92.83105	1945.746	88.52945	3979.36	181.3605052

Heat & Uncertainty

QB	Uncertainty Qb	QC	Uncertainty of Qc	QA	Uncertainty in QA
0.0552	1.1849	2.707	1.1371	2.7622	2.322
3.39584	1.1421	1.7109	1.0965	5.10674	2.2386
4.93872	1.1046	1.1539	1.0689	6.09262	2.1735
1.68016	1.1342	2.2339	1.0969	3.91406	2.2311

	Efficiency of B	Uncertainty	Efficiency of C	Uncertainty of C	Efficiency of A	Uncertainty of A
2	N/A	N/A	1.39124	0.587821	1.419609512	1.195119111
3	1.748743	0.593501	0.879303	0.564955	1.313590101	0.578921171
4	1.242293	0.283563	0.593037	0.550014	1.028944288	0.370048829
5	0.826194	0.559	1.148094	0.566158	0.983590381	0.56245728

References

[1] Engineering Toolbox, “Persons Heat Gain,” [Online]. Available: https://www.engineeringtoolbox.com/persons-heat-gain-d_242.html (accessed: Mar. 4, 2025).
[2] USU MAE Dept. “Heat Engine Lab Overview”, *MAE 4400 Canvas.* 2025
[3] International Electrotechnical Commission, "IEC Standard Voltages," [Online]. Available: https://webstore.iec.ch/preview/info_iec60038%7Bed7.0%7Db.pdf (accessed: Mar. 7, 2025).

AI Disclosure

Artificial Intelligence was used to edit this lab report, typeset the equations in TeX, and construct sections of the conclusion and abstract.